Angewandte Chemie
Eine Zeitschrift der Gesellschaft Deutscher Chemiker

Supporting Information

for

Angew. Chem. Int. Ed. Z53479

69451 Weinheim, Germany

A Novel Family of Supramolecular Frameworks of Polyconjugated Molecules Hosted in Aromatic Nanochannels

Piero Sozzani, Angiolina Comotti, Silvia Bracco, and Roberto Simonutti

Department of Materials Science, University of Milano Bicocca

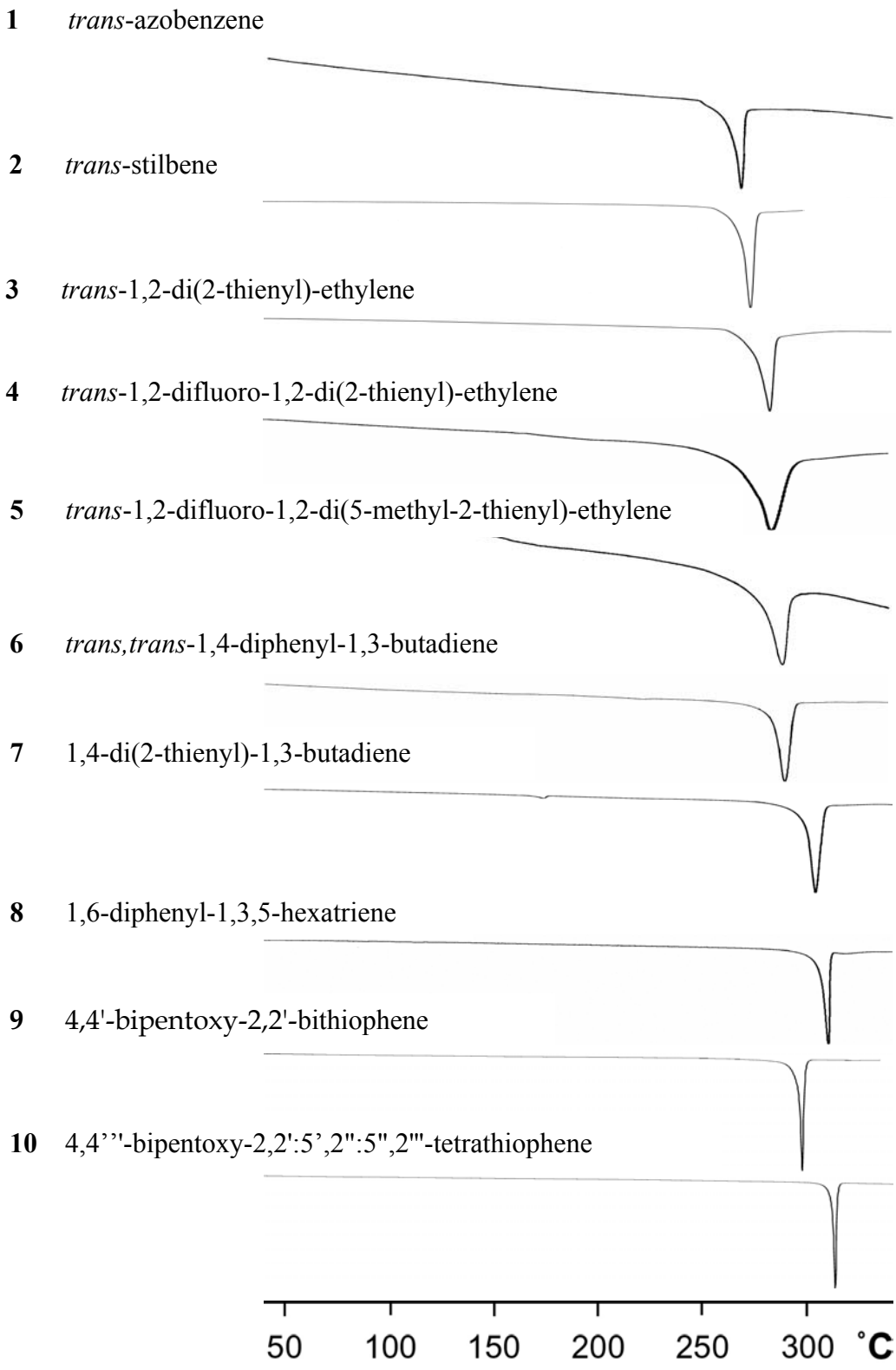

Figure S1. Differential scanning calorimetry of the adducts **1-10** indicated in the Table 1.

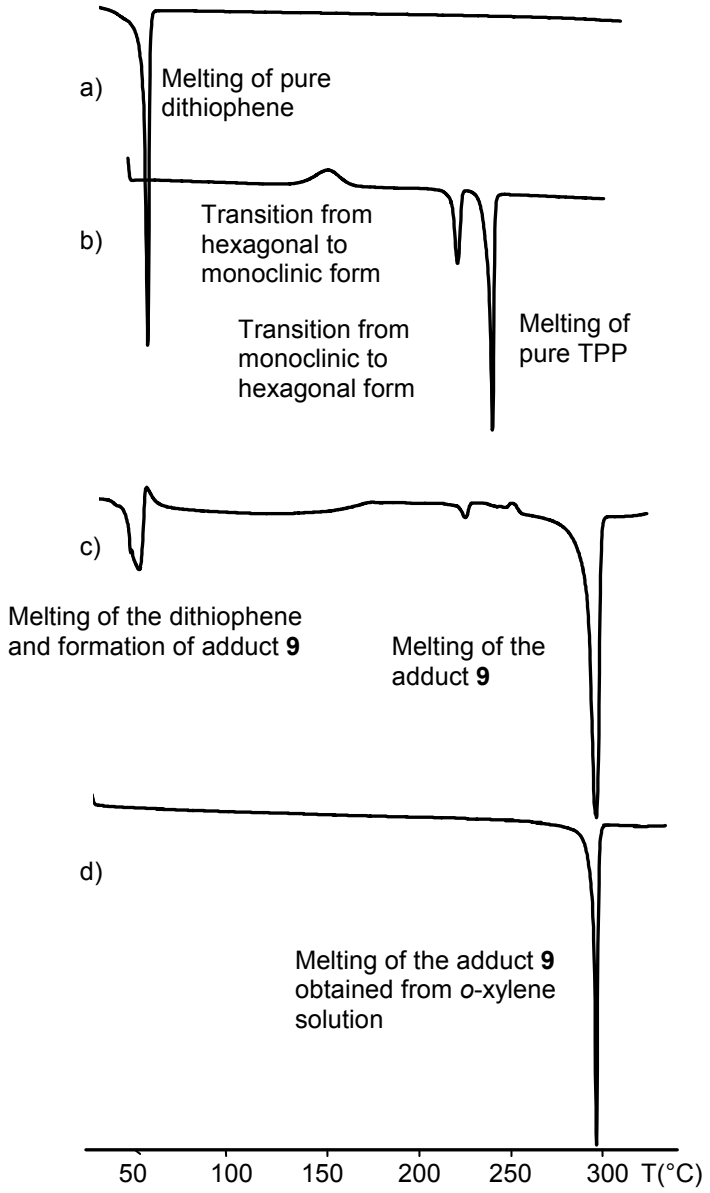

Figure S2. DSC traces of : a) pure 4,4'-dipentoxy-2,2'-dithiophene in the crystalline state; b) pure TPP matrix in the hexagonal form; c) a mechanical mixture of the dithiophene with the TPP matrix; d) adduct **9**. In the DSC trace of the mechanical mixture the formation of the adduct **9** is followed *in situ*: the melting of dithiophene is overlapped with the exotherm formation of the adduct **9**. At 230 and 250 °C the transitions of the TPP matrix disappear, instead a new peak at 296 °C is detected corresponding to the melting of the adduct **9**. The heating rate for all the traces is 10 °C/min. The DSC apparatus is a Mettler Toledo Star system.

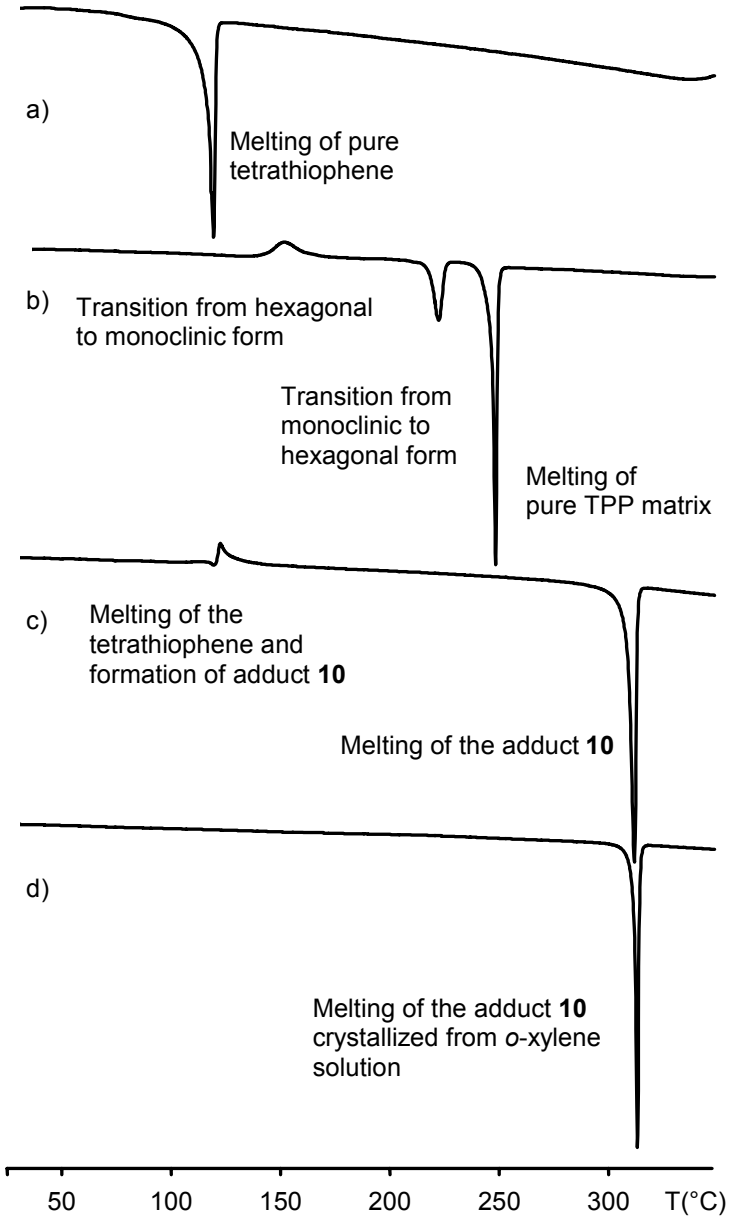

Figure S3. DSC traces of : a) pure 4,4'''-dipentoxy-2,2':5',2'':5'',2''':5''',2'''-tetrathiophene in the crystalline state; b) pure TPP matrix in the hexagonal form; c) a mechanical mixture of the tetrathiophene with the TPP matrix; d) adduct **10**. In the DSC trace of the mechanical mixture the formation of the adduct **10** is followed *in situ*: the melting of thiophene is overlapped with the exotherm formation of the adduct **10**. At 230 and 250 °C the transitions of the TPP matrix disappear, instead a new peak at 313 °C is observed corresponding to the melting of the adduct **10**. The heating rate for all the traces is 10 °C/min. The DSC apparatus is a Mettler Toledo Star system.

Crystal Data and structure refinement of compound 9

Space Group	$P6_3/m$
Wavelength	0.71073 Å
Crystal system	Hexagonal
Unit cell dimension	a=b= 11.627(1) Å
	c=10.084(1) Å
Volume	1180.7(2) $Å^3$
F(000)	480
Z	2
n. of frames	912
scan width	1.9 deg
exposure time	40 sec per frame
Crystal size	70 µm x 100 µm x 120 µm
Limiting indices	$-16 \leq h \leq 17$; $-16 \leq k \leq 17$; $-14 \leq l \leq 15$
Theta range for data collection	$3.5^o \div 32.3^o$
Reflection collected	35419
Observed reflections (I>3σ)	10314
Independent reflections	1365 (Rint 0.070)
Goodness of fit on F^2	2.51
Final R indices (I>3σ)	R1=0.0748, wR2=0.0192
R indices (all data)	R1=0.1685, wR2=0.0198

Table S1. Atomic Coordinates and isotropic displacement parameters for **9**.

Atom	x	y	Z	Uiso_eq
P1	0.64052(7)	0.18495(7)	0.25	0.0386(4)
O2	0.62237(10)	0.08562(10)	0.12865(9)	0.0447(6)
N3	0.52139(19)	0.21352(19)	0.25	0.0449(11)
C4	0.60600(16)	-0.03357(18)	0.17883(12)	0.0415(9)
C5	0.59333(18)	-0.14000(17)	0.10126(16)	0.0559(11)
C6	0.57944(19)	-0.24969(16)	0.17641(14)	0.0735(12)
C7	0	0	0	0.186(3)
C8	0	0	-0.1524(4)	0.247(3)

Table S2. Anisotropic displacement parameters ($Å^2$) for **9.**

Atom	U11	U22	U33	U12	U13	U23
P1	0.0486(5)	0.0380(5)	0.0309(4)	0.0228(4)	0	0
O2	0.0754(9)	0.0379(7)	0.0251(6)	0.0316(7)	0.0009(6)	0.0000(6)
N3	0.0368(13)	0.0398(14)	0.0570(13)	0.0183(12)	0	0
C4	0.0355(11)	0.0476(12)	0.0369(11)	0.0174(10)	-0.0007(8)	0.0157(9)
C5	0.0765(15)	0.0321(12)	0.0610(14)	0.0286(11)	0.0034(11)	-0.0103(11)
C6	0.0987(17)	0.0508(14)	0.0701(15)	0.0366(13)	-0.0042(11)	0.0008(10)

Table S3. Bond lengths (Å) for **9**.

Atoms	Distances
P1-P1i	2.7628(16)
P1-P1ii	2.7628(11)
P1-O2	1.6224(12)
P1-O2iii	1.6224(12)
P1-N3	1.578(3)
P1-N3ii	1.5803(19)
P1-C4	2.472(2)
P1-C4iii	2.472(2)
O2-O2iii	2.4473(12)
O2-N3	2.614(3)
O2-N3ii	2.624(2)
O2-C4	1.396(2)
O2-C4iii	2.3370(19)
O2-C5	2.487(3)
N3-N3i	2.706(3)
N3-N3ii	2.706(3)
C4-C4iii	1.4353(17)
C4-C5	1.408(3)
C4-C5iii	2.508(2)
C4-C6	2.374(3)
C4-C6iii	2.786(3)
C5-C5iii	3.000(2)
C5-C6	1.421(3)
C5-C6iii	2.544(2)
C6-C6iii	1.484(2)
S1-C20	1.537(4)
S1-C20iv	1.537(4)
C20-C20v	1.969(6)

(i)	1-x+y,1-x,1/2-z
(ii)	1+y,-x+y,-z
(iii)	x,y,1/2-z
(iv)	-x,-y,-z
(v)	-x+y,-x,-1/2-z

Table S4. Angles (°) for compound **9**.

O2-P1-O2	97.91(7)
O2-P1-N3	109.54(7)
O2-P1-N3	110.02(9)
N3-P1-N3	117.94(15)
P1-O2-C4	109.75(8)
P1-N3-P1	122.06(11)
O2-C4-C4	111.25(16)
O2-C4-C5	124.99(12)
C4-C4-C5	123.75(18)
C4-C5-C6	114.04(14)
C5-C6-C6	122.21(17)
C20-S1-C20	180
S1-C20-C20	180

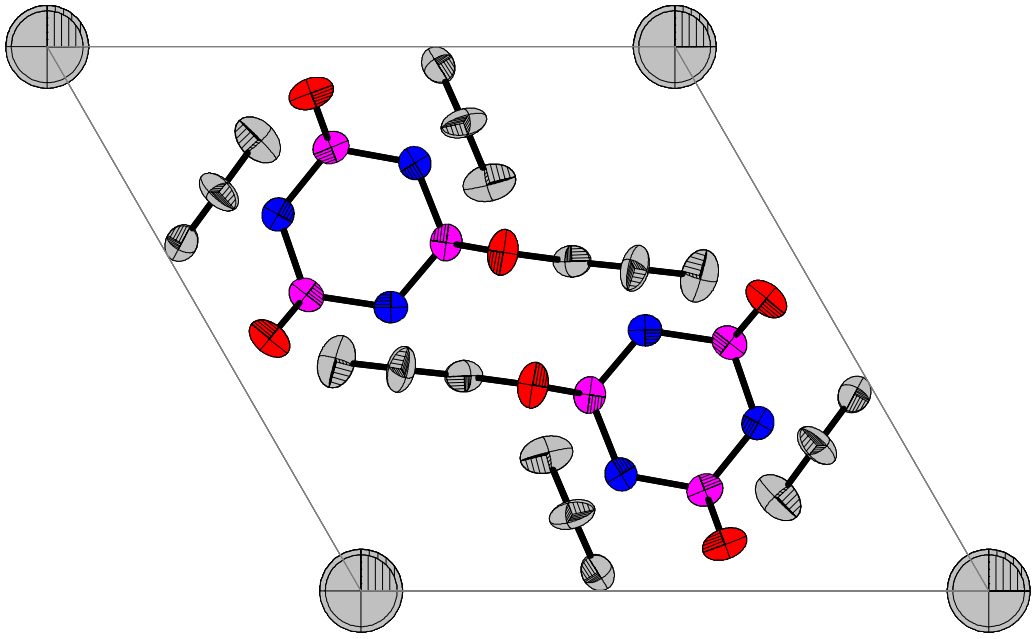

Figure S4. ORTEP drawing of **9**.

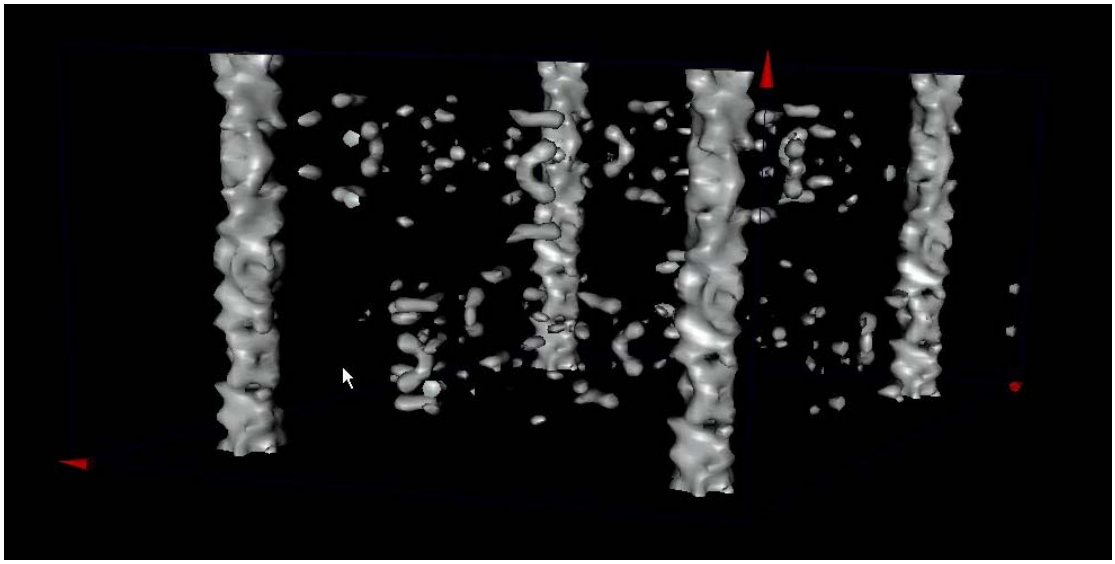

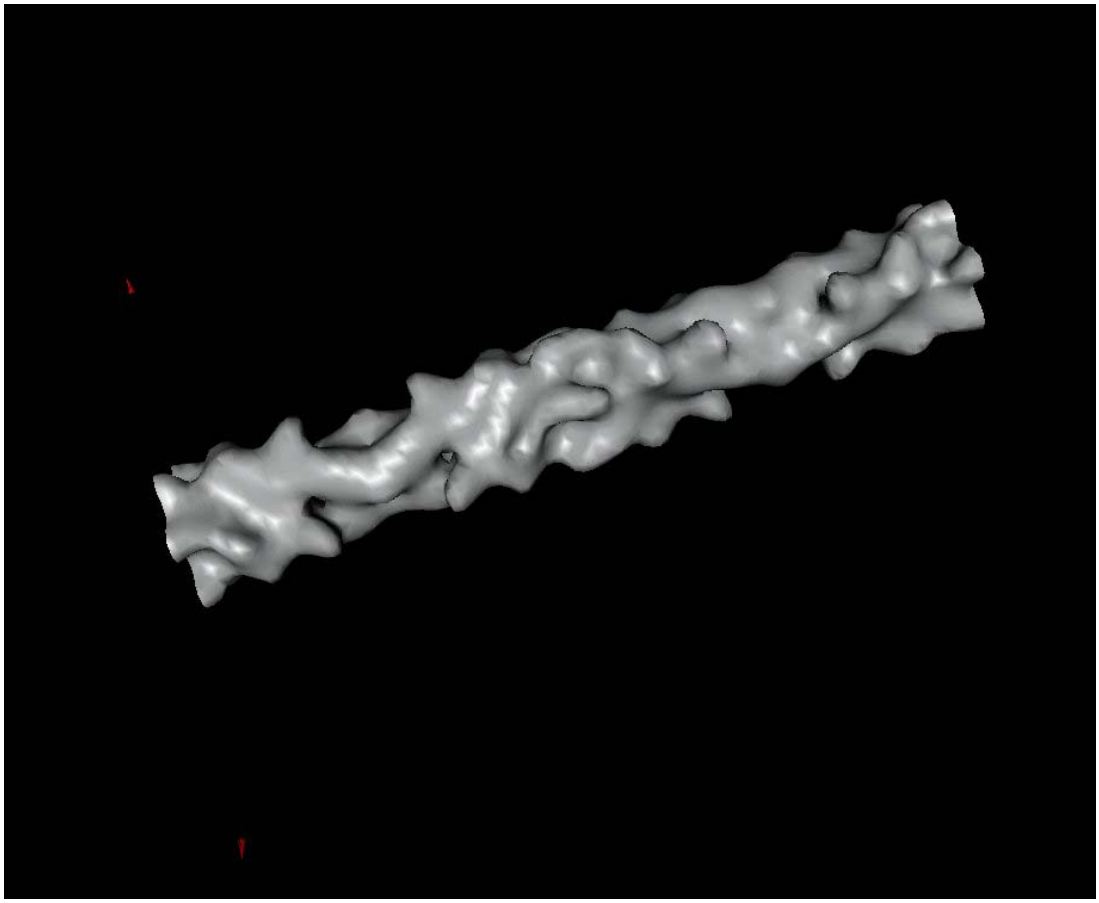

Figure S5. Residual electron density in the channels of **9**.

Crystal data and structural refinement of compound 10

Space Group	$P6_3/m$
Wavelength	0.71073 Å
Crystal system	Hexagonal
Unit cell dimension	a=b= 11.674(1) Å
	c=10.073(1) Å
Volume	1188.8(2) $Å^3$
F(000)	480
Z	2
n of frames	1158
scan width	1.5 deg
exposure time	40 sec per frame
Crystal size	100 µm x 120 µm x 150 µm
Limiting indices	$-16 \leq h \leq 17$; $-17 \leq k \leq 17$; $-14 \leq l \leq 14$
Theta range for data collection	4.5° ÷ 32.2°
Reflection collected	40391
Observed reflections (I>3σ)	6467
Independent reflections	1394 (Rint 0.13)
Goodness of fit	0.86
Final R indices (I>3σ)	R1=6.06, wR2=11.47
R indices (all data)	R1=27.94, wR2=13.95

Table S5. Atomic Coordinates and isotropic displacement parameters for **10**.

Atoms	x	y	z	Uiso eq
P1	0.64157(5)	0.18620(5)	0.75	0.0523(3)
O2	0.62520(7)	0.08703(7)	0.63035(6)	0.0607(5)
N3	0.52018(13)	0.21336(12)	0.75	0.0526(8)
C4	0.59210(11)	-0.13942(13)	0.60568(12)	0.0676(8)
C5	0.60792(11)	-0.03318(12)	0.68129(9)	0.0548(7)
C6	0.57482(13)	-0.24986(11)	0.68008(10)	0.0926(9)
C7	0	0	-0.4093(4)	0.283(2)
C8	0	0	-0.25	0.284(3)

Table S6. Anisotropic displacement parameters ($Å^2$) for **10**.

Atom	U11	U22	U33	U12	U13	U23
P1	0.0711(4)	0.0510(3)	0.0364(3)	0.0317(3)	0	0
O2	0.0999(6)	0.0584(5)	0.0308(4)	0.0449(5)	-0.0029(5)	-0.0045(4)
N3	0.0622(10)	0.0439(9)	0.0610(9)	0.0336(8)	0	0
C4	0.0924(10)	0.0515(9)	0.0631(10)	0.0392(8)	-0.0022(8)	-0.0148(8)
C5	0.0685(9)	0.0550(8)	0.0400(8)	0.0301(7)	0.0029(6)	0.0153(6)
C6	0.1442(13)	0.0664(10)	0.0679(10)	0.0532(10)	0.0021(8)	0.0158(7)

Table S7. Bond lengths (Å^2) for **10**.

Atoms	Distances
P1-P1i	2.7567(11)
P1-P1ii	2.7567(8)
P1-O2	1.6149(8)
P1-O2iii	1.6149(8)
P1-N3	1.5994(19)
P1-N3ii	1.5704(12)
P1-C5	2.4871(16)
P1-C5iii	2.4871(16)
O2-O2iii	2.4105(9)
O2-N3	2.6341(19)
O2-N3ii	2.5986(15)
O2-C4	2.4856(18)
O2-C5	1.4108(17)
O2-C5iii	2.3080(13)
N3-N3i	2.7336(17)
N3-N3ii	2.734(2)
C4-C4iii	2.9074(17)
C4-C5	1.387(2)
C4-C5iii	2.4388(17)
C4-C6	1.416(2)
C4-C6iii	2.4697(17)
C5-C5iii	1.3842(13)
C5-C6	2.360(2)
C5-C6iii	2.7423(19)
C6-C6iii	1.4086(15)
C7-C7iv	1.827(6)
C7-C8	1.605(4)

(i)	1-x+y,1-x,3/2-z
(ii)	1+y,-x+y,-z
(iii)	x,y,3/2-z
(iv)	-x,-y,-1-z

Table S8. Angles (°) for **10**.

O2-P1-O2	96.54(5)
O2-P1-N3	110.06(5)
O2-P1-N3	109.32(6)
N3-P1-N3	119.17(10)
N3-P1-N3	119.17(10)
P1-O2-C5	110.39(6)
P1-N3-P1	120.83(8)
P1-N3-P1	120.83(8)
C5-C4-C6	114.73(11)
O2-C5-C4	125.36(9)
O2-C5-C5	111.33(11)
C4-C5-C5	123.31(13)
C4-C6-C6	121.96(12)
C7-C7-C8	180
C7-C8-C7	180
C7-C8-C7	180

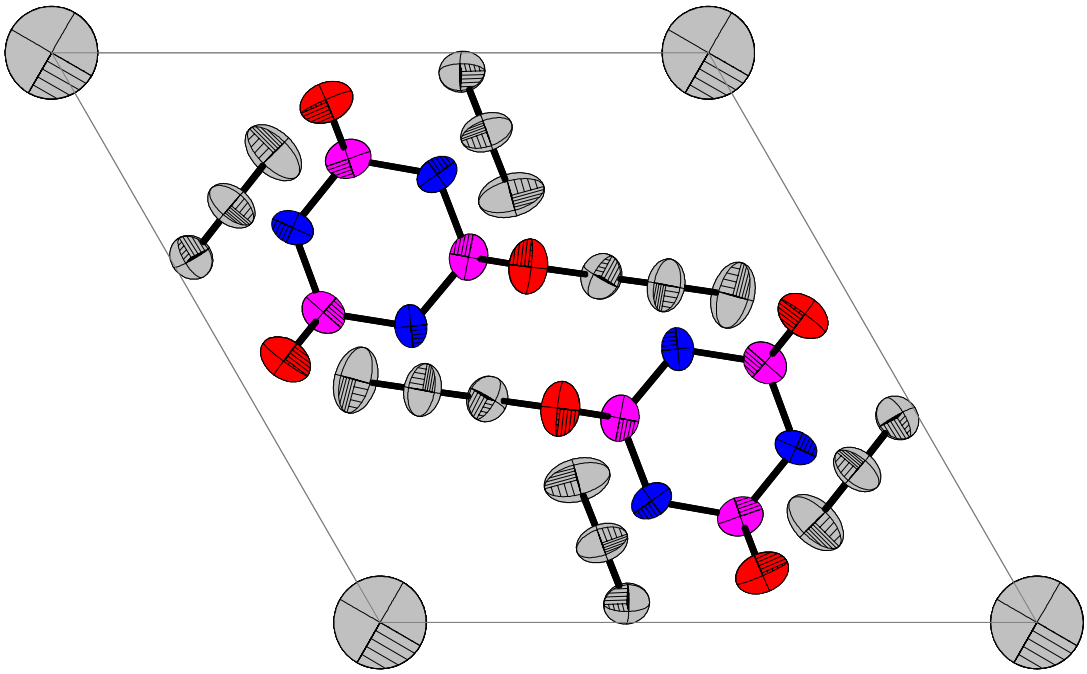

Figure S6. ORTEP drawing of the **10**.

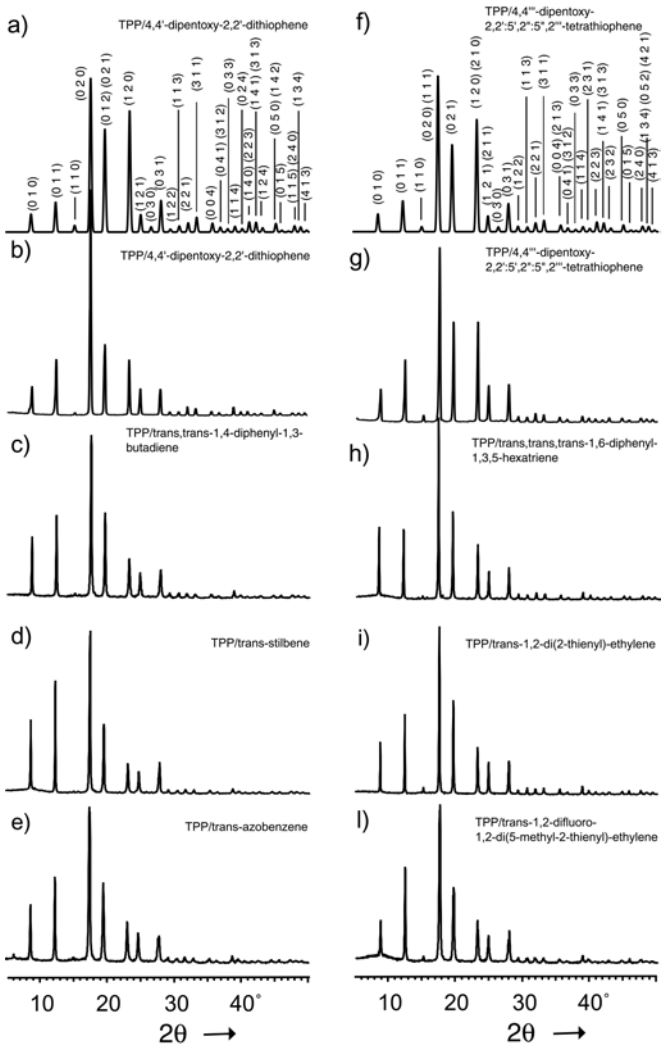

Figure S7. X-ray powder diffraction patterns and calculated profiles of the inclusion compounds with TPP. The peaks are indexed considering a hexagonal cell, space group $P6_3/m$ and taking into account the single-crystal X-ray solved structures (the same indexing reported in the calculated profiles is applied to all the spectra in the column). The unit-cell constants are refined by least-squares method from diffraction angles: a) compound **9**: calculated X-ray powder diffraction pattern of the structure as solved from single-crystal X-ray data; b) compound **9**: a=11.680(2) Å, c=10.113(7) Å, V=1194.915 Å^3; c) compound **6**: a=11.701(3) Å, c=10.094(5) Å, V=1196.848 Å^3; d) compound **2**: a=11.680(3) Å, c=10.084(5) Å, V=1191.389 Å^3; e) compound **1**: a=11.710(6) Å, c=10.11(1) Å, V=1200.413 Å^3; f) compound **10**: calculated X-ray powder diffraction pattern of the structure as solved from single-crystal X-ray data; g) compound **10**: a=11.708(4) Å, c=10.13(1) Å, V=1202.425 Å^3; h) compound **8**: a=11.648(1) Å, c=10.090(2) Å, V=1185.541 Å^3; i) compound **3**: a=11.661(2) Å, c=10.077(2) Å, V=1186.761 Å^3; l) compound **5**: a=11.711(3) Å, c=10.090(4) Å, V=1198.326 Å^3. Powder X-ray diffraction patterns were recorded using a Bruker D8 Advance diffractometer ($Cu_{K\alpha}$ radiation) in the 2θ range 5 to 60°, with $\Delta(2\theta)$=0.02° and 4 s per step as counting time.

Experimental NMR.

Phase-Modulated Lee-Goldburg (PMLG) heteronuclear (^{1}H-^{13}C) correlation (HETCOR) spectra were run at 75.5 MHz, on a Bruker Avance 300 instrument operating at a static field of 7.04 T. A MAS Bruker probe head was used with 4 mm ZrO_2 rotors spinning at a standard speed of 12.5 kHz. 90° pulse for proton was 2.9 μs. LG period was usually 18.9 μs. Quadrature detection in t_1 was achieved using TPPI method. RAMP-CP[1] is obtained changing the strength of the proton rf from 80 kHz at the beginning of the contact time to a value of 40 kHz at the end of the cross polarization period in 100 steps. Carbon signals (t_2) are acquired under proton decoupling, applying two pulse phase modulation scheme (TPPM)[2]. Particular care must be paid when the chemical shift values in F1 dimension are taken into account, since the chemical shift dispersion is scaled by a factor of $1/\sqrt{3}$ compared to what obtained in a directly detected ^{1}H spectrum. Moreover, a mismatch of the Lee-Goldburg condition might lead to a different scaling. Therefore, the chemical shift and the effectiveness of PMLG must be confirmed by a comparison to a ^{1}H spectrum.

NMR Background. Fast MAS (12.5 kHz spinning) averages the chemical shift anisotropy (CSA) of ^{13}C nuclei and practically reduces to zero the spinning side bands, reducing dramatically the complexity of the carbon spectrum, especially in systems containing carbons with large CSA as aromatic carbons. Multipulse decoupling schemes as CRAMPS techniques are not well suited for high spinning speed, in fact their complex pulse trains can be too long, compared with the rotor cycle, causing interference between the sample spinning and multipulse decoupling and an overall reduction of the effectiveness of decoupling. Thus, for obtaining a good proton homonuclear decoupling with fast MAS, Lee-Goldburg (LG) irradiation was successfully applied.[3] The full cycle time for LG decoupling is typically less then 20 μs and significantly shorter than the rotor period at spinning speed of 15 kHz. The key point of the Lee and Goldburg approach is the use of an *rf* field producing an effective field in the rotating frame inclined at the magic angle in respect to the static field. The fast precession of the spins about the magic-angle axis causes the zero-order average dipolar hamiltonian to vanish. In order to obtain a higher decoupling efficiency different strategies have been proposed, a rather effective sequence has been presented by Vega and co-workers[4]: in the so called phase-modulated Lee-Goldburg experiment (PMLG) the effective field at the magic angle is obtained by a series of adjacent phase shifted pulses. The pulse 2D ^{1}H-^{13}C HETCOR sequence used in this work exploits the PMLG approach and is reported in Figure S8.

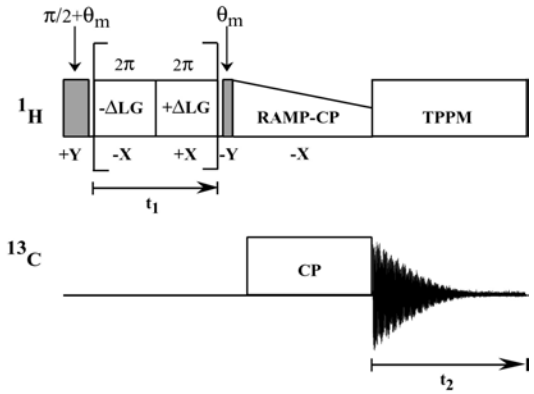

Figure S8. A $(\pi/2+\theta_m)_y$ preparation pulse puts the ^{1}H polarization perpendicular to *z* axis of the effective field in the tilted rotating frame, during t_1 a PMLG irradiation sequence is applied. At the end of t_1 a θ_m pulse brings back the magnetization into the xy plane. In order to have an efficient transfer of magnetization to the carbon nuclei under fast MAS during the contact time a RAMP-CP is applied, this procedure restores a broader matching profile between proton and carbon nuclei. During acquisition TPPM heteronuclear decoupling is applied.

References:
(1) G. Metz, X. Wu, S. O. Smith, *J. Magn. Reson. A* **1994**, *110*, 219-227.
(2) A. E. Bennet, C. M. Rienstra, M. Auger, K. V. Lakshmi, R. G. Griffin, *J. Chem. Phys.* **1995**, *103*, 6951-6958.
(3) B.-J. Van Rossum, H. Förster, H. J. M. de Groot, *J. Magn. Reson.* **1997**, *124*, 516-519.
(4) E. Vinogradov, P. K. Madhu, S. Vega, *Chem. Phys. Lett.* **1999**, *314*, 443-450.

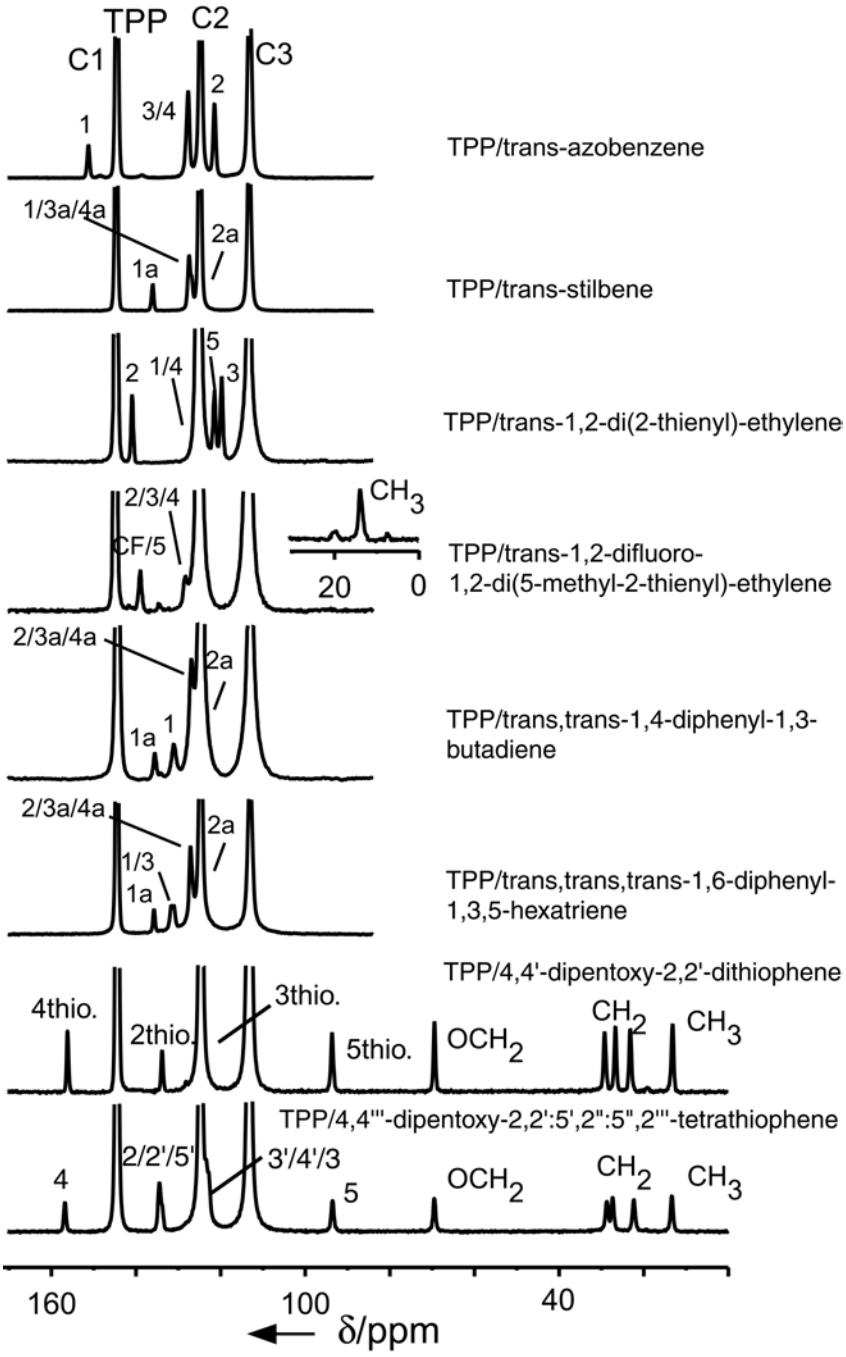

Figure S9. ^{13}C Ramped-CP MAS NMR spectra of the adducts. The spectra were performed under a spinning speed of 15 kHz. The chemical shift values of the adducts are reported below.
1: ^{13}C NMR (75.46 MHz, CP MAS): δ = 151.29 (C-1), 144.57 (C-1 of TPP), 127.73 (C-3, C-4), 124.78 (C-3 of TPP), 121.49 (C-2), 113.21 (C-2 of TPP). Bulk trans-azobenzene: ^{13}C NMR (75.46 MHz, CP MAS): δ = 153.81/152.90 (C-1), 130.39/128.87 (C-4, C-3), 118.11/116.85 (C-2).

2: ^{13}C NMR (75.46 MHz, CP MAS): δ = 144.96 (C-1 of TPP), 136.32 (C-1a), 127.71/127.17 (C-1, C-3a, C-4a), 125.18 (C-2a, C-3 of TPP), 113.53 (C-2 of TPP). Bulk trans-stilbene: ^{13}C NMR (75.46 MHz, CP MAS): δ = 137.68 (C-1a), 130.18 (C-1, C-3a), 128.60 (C-4a), 125.14 (C-2a).
3: ^{13}C NMR (75.46 MHz, CP MAS): δ = 144.83 (C-1 of TPP), 141.08 (C-2thio.), 125.86 (C-1, C-4thio., C-3 of TPP), 121.60 (C-5thio.), 119.91 (C-3thio.), 113.51 (C-2 of TPP). Bulk trans-1,2-di(2-thienyl)-ethylene: ^{13}C NMR (75.46 MHz, CP MAS): δ = 144.15 (C-2thio.), 129.20/127.97 (C-1thio., C-4thio.), 125.20 (C-5thio.), 123.21 (C-3thio.).
4: Bulk trans-1,2-difluoro-1,2-di(2-thienyl)-ethylene: ^{13}C NMR (75.46 MHz, CP MAS): δ = 144.38 (=C-F), 131.60 (C-2thio.), 128.71 (C-4thio.), 127.35 (C-5thio.), 125.47 (C-3thio.).
5: ^{13}C NMR (75.46 MHz, CP MAS): δ = 144.92 (C-1 of TPP), 141.76 (=C-F, C-5thio.), 125.22 (C-2thio., C-3thio., C-4thio., C-3 of TPP), 113.75 (C-2 of TPP), 13.87 (CH_3). Bulk trans-1,2-difluoro-1,2-di(5-methyl-2-thienyl)-ethylene: ^{13}C NMR (75.46 MHz, CP MAS): δ = 144.30/143.16 (=C-F, C-5thio.), 128.82 (C-2thio., C-4thio.), 124.52 (C-3thio.), 15.96 (CH_3).
6: ^{13}C NMR (75.46 MHz, CP MAS): δ = 144.70 (C-1 of TPP), 135.89 (C-1a), 131.38 (C-1), 127.25 (C-2, C-3a, C-4a), 124.99 (C-2a, C-3 of TPP), 113.37 (C-2 of TPP). Bulk trans,trans-1,4-diphenylene-1,3-butadiene: ^{13}C NMR (75.46 MHz, CP MAS): δ = 137.02 (C-1a), 134.33/132.68 (C-1), 129.41 (C-2, C-3a, C-4a), 125.36 (C-2a).
7: Bulk 1,4-di(2-thienyl)-1,3-butadiene: ^{13}C NMR (75.46 MHz, CP MAS): δ = 145.08/143.00 (C-2thio.), 129.59 (C-1, C-4thio., C-2), 127.71 (C-5thio.), 126.48 (C-3thio.).
8: ^{1}H NMR (300.13 MHz, MAS): δ = 7.02 (12 H, CH of TPP), 5.61 (4 h, 2a-H, 3a-H, 4a-H, 2-H), 4.74/4.61 (2 H, 1-H, 3-H); ^{13}C NMR (75.46 MHz, CP MAS): δ = 144.73 (C-1 of TPP), 135.99 (C-1a), 131.89 (C-3), 131.32 (C-1), 127.35 (C-2, C-3a, C-4a), 124.92 (C-2a, C-3 of TPP). Bulk Diphenylenehexatriene: ^{1}H NMR (300.13 MHz, MAS): δ = 6.57 (3 H, 2a-H, 3a-H, 4a-H); ^{13}C NMR (75.46 MHz, CP MAS): δ = 136.76 (C-1a), 135.29/134.63/132.79 (C-1, C-3), 129.48 (C-2, C-3a, C-4a), 125.00 (C-2a).
9: ^{1}H NMR (300.13 MHz, MAS): δ = 7.04 (12 H, CH of TPP), 4.10 (4 H, 3-H, 3'-H, 5-H, 5'-H; CH of thiophene rings), 1.80 (4 H, O-CH_2), -1.08 (18 H; 6 CH_2 and 2 CH_3); ^{13}C NMR (75.46 MHz, CP MAS): δ = 156.47 (C-4, C-4'), 144.71 (C-1 of TPP), 134.04 (C-2, C-2'), 124.86 (C-3 of TPP), 113.31 (C-3, C-3', C-2 of TPP), 93.72 (C-5, C-5'), 69.42 (2 O-CH_2), 29.06/26.49/22.99 (6 CH_2), 12.93 (2 CH_3). Bulk Dithiophene: ^{1}H NMR (300.13 MHz, MAS): δ = 6.20 (4 H, 3-H, 3'-H, 5-H, 5'-H; CH of thiophene rings), 3.61 (4 H, O-CH_2), 1.12/0.76/0.14 (18 H; 6 CH_2 and 2 CH_3); ^{13}C NMR (75.46 MHz, CP MAS): δ = 157.25 (C-4, C-4'), 137.94 (C-2, C-2'), 114.98 (C-3, C-3'), 95.77 (C-5, C-5'), 70.85 (2 O-CH_2), 33.21/29.51/25.16 (6 CH_2), 16.24 (2 CH_3).
10: ^{1}H NMR (300.13 MHz, MAS): δ = 7.16 (12 H, CH of TPP), 5.59/3.96 (4 H, 3-H, 3'-H, 4'-H, 5 H; CH of thiophene rings), 1.88 (2 H; O-CH_2), -0.94 (9 H; 3 CH_2 and 1 CH_3); ^{13}C NMR (75.46 MHz, CP MAS): δ = 157.14 (C-4), 144.80 (C-1 of TPP), 134.71/134.04 (C-2, C-2', C-5'), 124.94 (C-3 of TPP), 123.66/123.04 (C-3', C-4'), 113.36 (C-3, C-2 of TPP), 93.63 (C-5), 69.46 (O-CH_2), 28.51 (CH_2), 27.15 (CH_2), 22.11 (CH_2), 13.09 (CH_3). Bulk Tetrathiophene: ^{1}H NMR (300.13 MHz, MAS): δ = 6.47 (3 H, 3-H, 3'-H, 4'-H), 5.63 (1 H, 5-H), 3.45 (2 H, O-CH_2), 0.99/0.68 (9 H; 3 CH_2 and 1 CH_3); ^{13}C NMR (74.46 MHz, CP MAS): δ = 158.67 (C-4), 136.03 (C-2, C-2', C-5'), 123.90/122.57 (C-3', C-4'), 116.90 (C-3), 95.69 (C-5), 71.31 (1 O-CH_2), 31.69/31.26/24.83 (3 CH_2), 15.91 (1 CH_3).
The assignments are given with respect to the submolecular asymmetric unit because of the symmetry of the molecules.

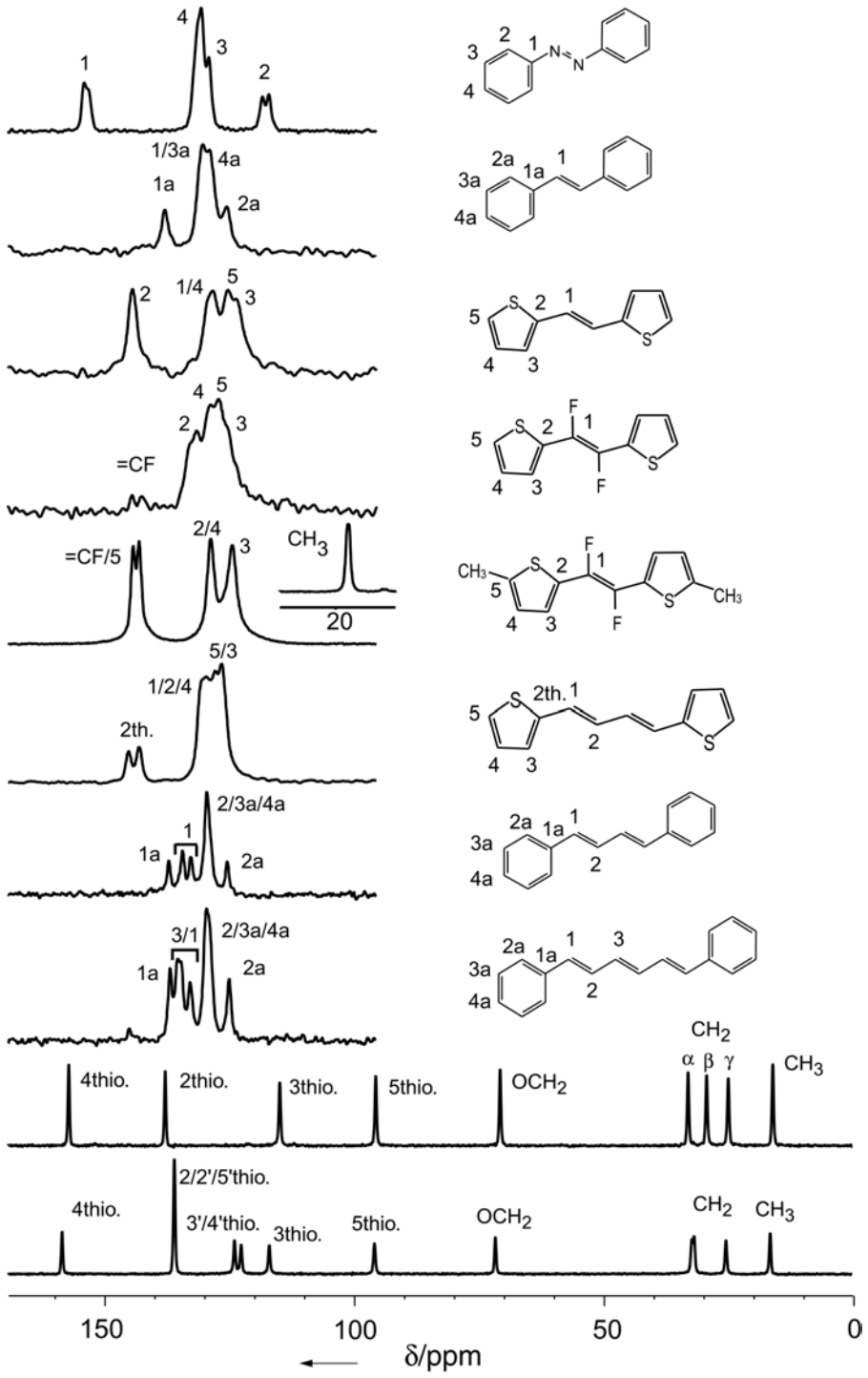

Figure S10. ^{13}C Ramped-CP MAS NMR spectra of the crystalline phases of molecules in bulk. The spectra were performed under a spinning speed of 15 kHz. The chemical shift values are reported in the Experimental Section. The chemical shifts of the molecules in $CDCl_3$ solution are the following: trans-azobenzene: ^{13}C NMR (50.23 MHz in $CDCl_3$): δ = 152.66 (C-1), 130.94 (C-4), 129.04 (C-3), 122.84 (C-2); trans-stilbene: ^{13}C NMR (50.23 MHz in $CDCl_3$): δ = 137.36 (C-1a), 128.67 (C-1, C-3a), 127.61 (C-4a), 126.53 (C-2a); trans-1,2-difluoro-1,2-di(2-thienyl)-ethylene: ^{13}C NMR (50.23 MHz in $CDCl_3$): δ = 144.7 (dd, J_{CF1}=275.5 Hz, J_{CF2}=92.6 Hz, =CF), 131.7 (t, J_{CF1}=9.25Hz, J_{CF2}=9.25Hz, C-2thio.), 128.0 (s, C-4thio.), 127.8 (t, J_{CF1}=3.7Hz, J_{CF2}=3.7Hz, C-5thio.), 125.8 (t, J_{CF1}=3.7Hz, J_{CF2}=3.7Hz, C-3thio.); trans,trans-1,4-diphenylene-1,3-butadiene: ^{13}C NMR (50.23 MHz in $CDCl_3$): δ = 137.38 (C-1a), 132.83 (C-1), 129.26 (C-2), 128.66 (C-3a), 127.56 (C-4a), 126.39 (C-2a); diphenylenehexatriene: ^{1}H NMR (400 MHz in $CDCl_3$): δ = 7.41 (1 H, 2a-H), 7.32 (1 H, 3a-H), 7.23 (1 H, 4a-H), 6.88 (1 H, 2-H), 6.60 (1 H, 1-H), 6.52 (1 H, 3-H); ^{13}C NMR (50.23 MHz in $CDCl_3$): δ = 137.40 (C-1a), 133.57 (C-3), 132.69 (C-1), 129.13 (C-2), 128.64 (C-3a), 127.53 (C-4a), 126.37 (C-2a); dithiophene: ^{1}H NMR (50.23 MHz in $CDCl_3$): δ = 6.83 (d, J=1.71 Hz, 2 H, 3-H, 3'-H), 6.12 (d, J=1.71Hz, 2 H, 5-H, 5'-H), 3.94 (t, J=6.3 Hz, 4 H, O-CH_2), 1.95-0.81 (18 H; 6 CH_2 and 2 CH_3); ^{13}C NMR (50.23 MHz in $CDCl_3$): δ = 158.03 (C-4, C-4'), 136.49 (C-2, C-2'), 116.33 (C-3, C-3'), 96.80 (C-5, C-5'), 70.59 (2 O-CH_2), 29.41/28.67/22.94 (6 CH_2),

14.49 (2 CH_3); tetrathiophene: ^{1}H NMR (50.23 MHz, in $CDCl_3$): δ = 7.10-7.02 (pseudo singlet, 4 H, 3'-H, 3''-H, 4'-H, 4''-H), 6.85 (d, J=6.2 Hz, 2 H, 3-H, 3'''-H), 6.14 (d, J= 1.60 Hz, 2 H, 5-H, 5'''-H), 3.96 (t, J=6.2 Hz, 4 H, O-CH_2), 1-87-0.90 (18 H; 6 CH_2 and 2 CH_3); ^{13}C NMR (50.23 MHz in $CDCl_3$): δ = 158.79 (C-4, C-4'''), 137.68 (C-2, C-2'''), 137.10 (C-5', C-5''), 136.46 (C-2', C-2''), 125.34/125.24 (C-3', C-3'', C-4', C-4''), 117.14 (C-3, C-3'''), 97.5 (C-5, C-5''').

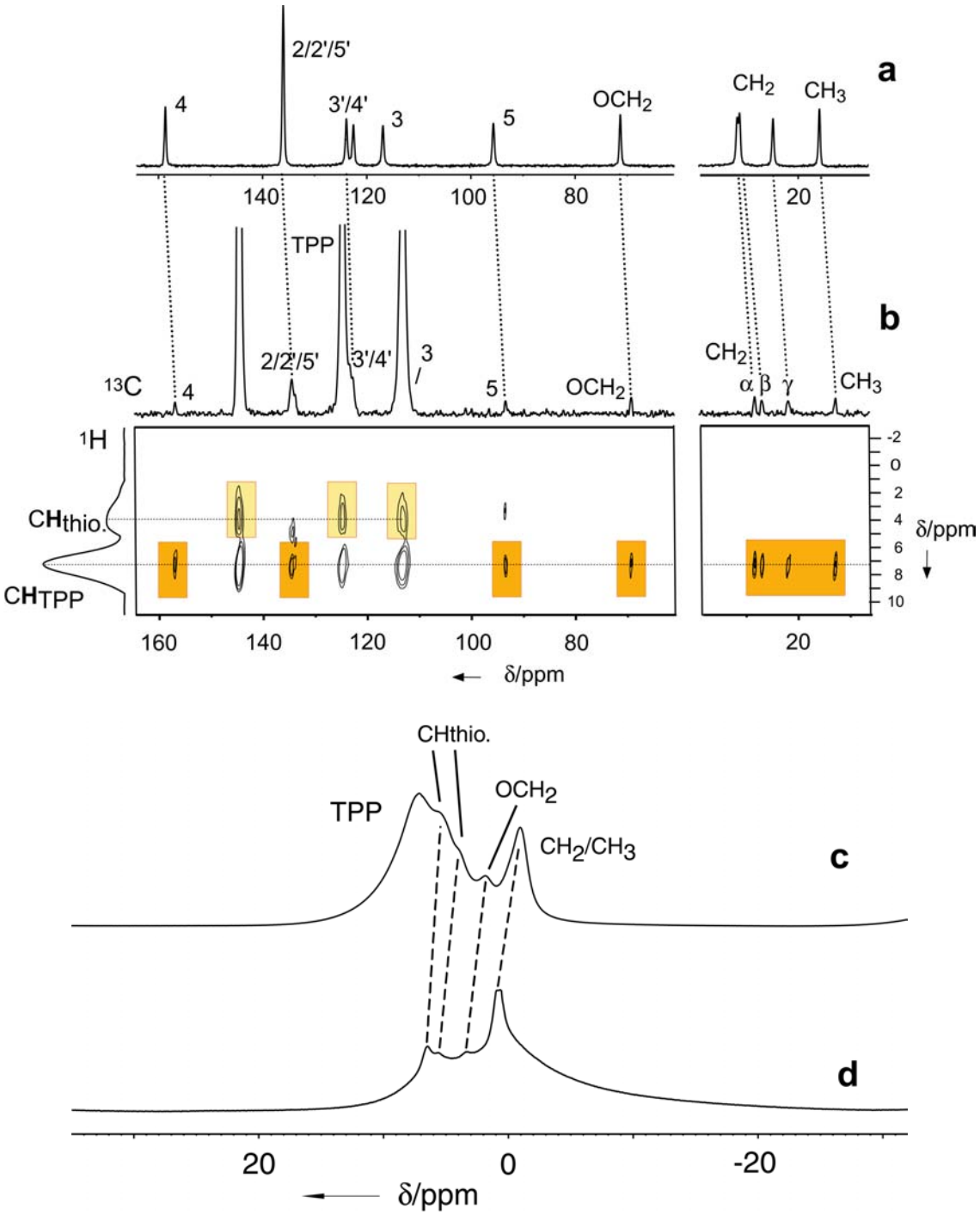

Figure S11. a) ^{13}C Ramped-CP MAS NMR spectrum the 4,4'''-dipentoxy-2,2':5',2'':5'',2'''-tetrathiophene. b) Contour plots of 2D Phase-Modulated Lee-Goldburg PMLG decoupled heteronuclear (^{1}H-^{13}C) dipolar correlation spectrum from compound **10**. The spectra were performed in a magnetic field of 7.04 T using a spinning speed of 15 kHz. Ramped-CP times of a) 1ms and b) 5 ms were applied. ^{1}H MAS NMR spectrum under 15 kHz spinning speed of c) the compound **10** and d) the pure 4,4'''-dipentoxy-2,2':5',2'':5'',2'''-tetrathiophene in the crystalline state.